Journal of Computational Neuroscience 11, 241–248, 2001

Independent Component Analysis of Temporal Sequences Subject to Constraints by Lateral Geniculate Nucleus Inputs Yields All the Three Major Cell Types of the Primary Visual Cortex

BOTOND SZATMÁRY AND ANDRÁS LŐRINCZ
Department of Information Systems, Eötvös Loránd University, Pázmány Péter sétány 1/C, Budapest, Hungary H-1117
botond@inf.elte.hu
lorincz@inf.elte.hu

Received May 18, 2001; Revised September 26, 2001; Accepted October 10, 2001

Action Editor: Jonathan D. Victor

Abstract. Information maximization has long been suggested as the underlying coding strategy of the primary visual cortex (V1). Grouping image sequences into blocks has been shown by others to improve agreement between experiments and theory. We have studied the effect of temporal convolution on the formation of spatiotemporal filters—that is, the analogues of receptive fields—since this temporal feature is characteristic to the response function of lagged and nonlagged cells of the lateral geniculate nucleus. Concatenated input sequences were used to learn the linear transformation that maximizes the information transfer. Learning was accomplished by means of principal component analysis and independent component analysis. Properties of the emerging spatiotemporal filters closely resemble the three major types of V1 cells: simple cells with separable receptive field, simple cells with nonseparable receptive field, and complex cells.

Keywords: sign-changing filters, complex filters, temporal convolution, temporal sequences, independent component analysis

1. Introduction

It has been argued (Attneave, 1954; Barlow, 1972; Field, 1987) that the visual cortex may filter sensory information with the help of factorial code. The used filters would code independent properties of natural scene ensembles. This issue is well studied in the primary visual cortex, which contains a large variety of receptive fields (RFs). As it is widely known, most of these RFs respond vigorously to elongated bars or edges (Hubel and Wiesel, 1959). The factorial code assumption is supported by recent computational advances. Several studies demonstrated that a variety of information transfer optimizing algorithms give rise to RF properties similar to those of simple cells of the primary visual cortex. Sparse coding (Olshausen and Field, 1996, 1997) and independent component (IC) analysis (ICA) (Bell and Sejnowski, 1997) are the two major methods to be mentioned here. ICA also seems to be powerful in generating color opponent receptive fields (Tailor et al., 2000). Hateren and Ruderman (1998) argue that IC analysis of *temporal* sequences (TICA) instead of static images may result in even better similarities. They used natural images sequences and grouped those into blocks. This way they could develop temporal filters, which are nonseparable alike to spatiotemporal RFs found experimentally (DeAngelis et al., 1993) and covered a range of spatial and temporal

frequencies. From an information theoretic point of view the idea of grouping inputs into blocks is appealing: it is known that combining (for example, concatenating) signals into larger groups may help cope with the channel capacity constraints (Cover and Thomas, 1991). In other words, grouping may speed up the information flow. Biological considerations also support the view that long-term memory formation is based on the analysis of temporal sequences rather than using only single inputs (Lisman and Idiart, 1995; Lisman, 1999).

In choosing among models, it is a falsifying issue for the information maximization principle whether it can produce all major types of RFs of the V1 or not. There are two types of RFs that—to our knowledge—have not yet been produced by a *single* algorithm working with information maximization procedures: separable time-dependent RFs that have optimal excitation that changes sign in space and time (DeAngelis et al., 1993, 1999) and complex RFs (Sillito, 1979; Henry et al., 1983; Hammond, 1991; Mignard and Malpeli, 1991; Zigmund et al., 1999). The lack of the emergence of these filters as a result of IC analysis could question the importance of factorial coding.

According to the model of Wimbauer et al. (1997), spatiotemporal filters bridging 100 ms or so can be formed in the V1 because of the presence of four different input types that converge onto the cortical cells. The four types of input correspond to nonlagged ON and OFF inputs and lagged ON and OFF inputs. The response function of nonlagged and lagged cells can be estimated (Wimbauer et al., 1997) by using the power spectrum of the cell response (Saul and Humphrey, 1990) and information theoretic principles (Dong and Atick, 1995). The response function has heavy tails (Cai et al., 1997), which may have a strong impact on receptive field properties. This noninstantaneous response function corresponds to temporal convolution (temporal smoothing) of inputs. Temporal convolution of the visual information has to be considered in modeling receptive fields of V1. Another issue of spatiotemporal filter (STF) formation is the limitation of the number of computational units (cells) posed, such as by the columnar organization. In this article STF formation is studied as a function of the degree of temporal convolution *and* the number of available computational units. Principal component analysis (PCA) (Pearson, 1901; Hotteling, 1933; Haykin, 1994) is used to decrease (compress) the number of computational units available for information transfer. PCA was used here in the same way as it was used by van Hateren and van der Schaaf (1998). Elaborated examples of PCA applications can be found in the literature (Buchsbaum and Gottschalk, 1983). Reducing the number of computational units corresponds the limited numbers of V1 cells in micro-columns (Calvin, 1999) relative to the number of converging lateral geniculate nucleus (LGN) cells. This ratio is a function of cell type and topographical organization in V1. The present work extends the preliminary study of Lőrincz et al. (2000) and intends to offer some advances over other models of receptive fields in V1.

2. Methods

Static natural images and movies (i.e., image streams) on a car moving on highway and in city traffic were used in our work. For static images, inputs ($\mathbf{x}$) were formed by *concatenating* small windows placed to *different* position along a randomly chosen straight line on a larger image. This case corresponds to a *translating gaze* in a still environment. For image streams, inputs ($\mathbf{x}$) were constructed by concatenating small windows placed to the *same* position but on *consecutive* images. This case corresponds to *fixed gaze* in a moving environment. We note that the two data types (natural scene and highway traffic) have different statistical properties. In both cases we used a window of 13×13 pixels arranged on a hexagonal grid for sampling. Pixel values of the window (sampling points) were interpolated from neighboring image pixels of the square grid of the original image. The distance between nearest neighbor pixels on the hexagonal grid and on the images were approximately equal. This sampling method avoids artifacts that could arise for orthogonal grids (Olshausen and Field, 1996). For both types of input generation inputs and input components can be indexed with time:

$$\mathbf{x}(t) = (x(t),\ x(t-1), \ldots, x(t-n+1)),$$

where n is the number of concatenated patches. In our work n was 7, and therefore the dimension of $\mathbf{x}$ was equal to $7 \cdot 13 \cdot 13 = 1183$. The concept of input concatenation and input component arrangement are depicted in Fig. 1 for the case of translating gaze.

For the moving gaze case, the motion directions were pooled with uniform distribution in the sampling procedure. For the moving environment case, the position of the filter at the first frame was randomly chosen and then remained constant.

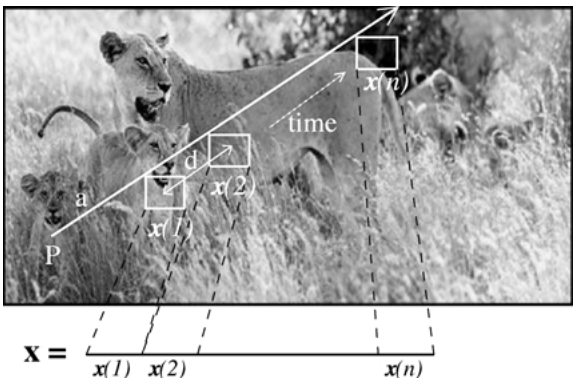

Figure 1. Making of the input on the natural scene. A square window from an arbitrarily chosen P point was translated along a randomly chosen straight line a. The window was made of 13×13 sampling points arranged on a hexagonal grid. Pixel values of the window were interpolated from the original image. The distance between the nodes of the hexagonal grid was equal to 1 in units of pixel distance on the original image. The positioning of the windows on the image correspond to consecutive sampling positions. The distance between these positions, d, defines the window distance. The vector $\mathbf{x}$ contains the list-ordered 169 pixel values of each consecutive frames $(x(1), \ldots, x(n), n = 7)$ along the patches. Independent component analysis was performed on temporally smoothened $\mathbf{x}$ vectors.

For both static images and movie scenes, temporal convolution (smoothing) induced by exponential kernels—also called leaky integration—was studied. Note that temporal convolution is a special kind of mixing; it mixes input components of different temporal indices and produces an *effective* input $\mathbf{y}(t)$. Inputs $\mathbf{x}(t)$ belonging to different time indices were weighted by a geometrical series λ^{t-k} and were added up:

$$\mathbf{y}(t) = \sum_{k=1}^{t} \mathbf{x}(t) \exp((t-k)\ln\lambda) = \sum_{k=1}^{t} \mathbf{x}(k)\lambda^{t-k},$$

where $0 \leq \lambda < 1$ is the convolution parameter. For a review on convolution, see Graham et al. (1989). The influence of earlier inputs diminishes according to the geometric series, while the most recent input $(k = t)$ has the strongest impact on forming $\mathbf{y}(t)$. When $\lambda = 0$, only the $k = t$ term remains, which corresponds to inputs with no temporal convolution. The word *convolution* concerns the opposing temporal dependence of the two functions of the series: the time arguments change linearly and the sum of the arguments $(k + (t-k))$ is constant. In order to avoid transients in the convolution operation, inputs with small t values (smaller than $3 \cdot \lceil(-1/\ln(\lambda))\rceil$, where $\lceil\cdot\rceil$ rounds the argument to the nearest integer greater than or equal to the argument) were excluded from the training set. For reproducibility reasons we used the parameter free FastICA algorithm (Havärinen and Oja, 1997). The number of inputs was 7000. PCA transformation was used to study information transfer in important subspaces of the input space. The reduced dimensional PCA subspace minimizes the loss of information in mean square error over the full data set.

IC analysis was applied on the input set $\mathbf{y}(t)$ $(t = 1, 2, \ldots, 7000)$ to linearly transform the input space. ICA is based on the following assumption: the input $(\mathbf{y})$ is composed from an unknown set of source signals $\mathbf{s} = (s_1, \ldots, s_m)$ originating from independent sources, mixed by an unknown mixing matrix $\mathbf{A}$, and covered by noise: $\mathbf{y} = \mathbf{A}\mathbf{s}' + \texttt{noise}$, where a row vector with prime denotes its column vector form. The goal of the IC analysis is to develop the separating matrix $\mathbf{W}$ that inverts the mixing matrix $\mathbf{A}$: $\mathbf{WA} = \mathbf{I}$, where matrix $\mathbf{I}$ is the identity matrix of the reduced dimensional PCA subspace. The rows of matrix $\mathbf{W}$ form the independent component filters (ICFs). Components of the linearly transformed inputs convey minimum mutual information and are as independent of each other as possible. Applying ICA to temporal sequences, the resulting ICF basis set is made of STFs with minimized mutual information. For a review on ICA, see Hyvärinen (1999b).

3. Results

Some representative ICFs are shown in Fig. 2 as a function of the convolution parameter λ. The dimension of the ICF vectors and the inputs are equal. Components of the ICFs correspond to pixels. Pixels have spatial indices (from 1 to 169) and temporal indices (from 1 to 7). In order to visualize ICFs, pixels of the same temporal indices were collected into a frame and were rearranged according to their original positions. Each ICF corresponds to a frame sequence. A frame sequence represents a spatiotemporal filter. It is worth noting that the resulting filter image sequence is equal to the optimal input series belonging to the filter: this image stream can best stimulate the filter. In figures, frames of the sequences are time ordered: time increases from left (the first frame) to the right (the last frame). Each 13×13 value of a frame corresponds to a node of the hexagonal grid. For presentational purposes the values of the hexagonal grid are interpolated between the nodes by nearest neighbor averaging. The applied PCA dimension is 169; thus the number of ICFs is 169 ($\ll$1183).

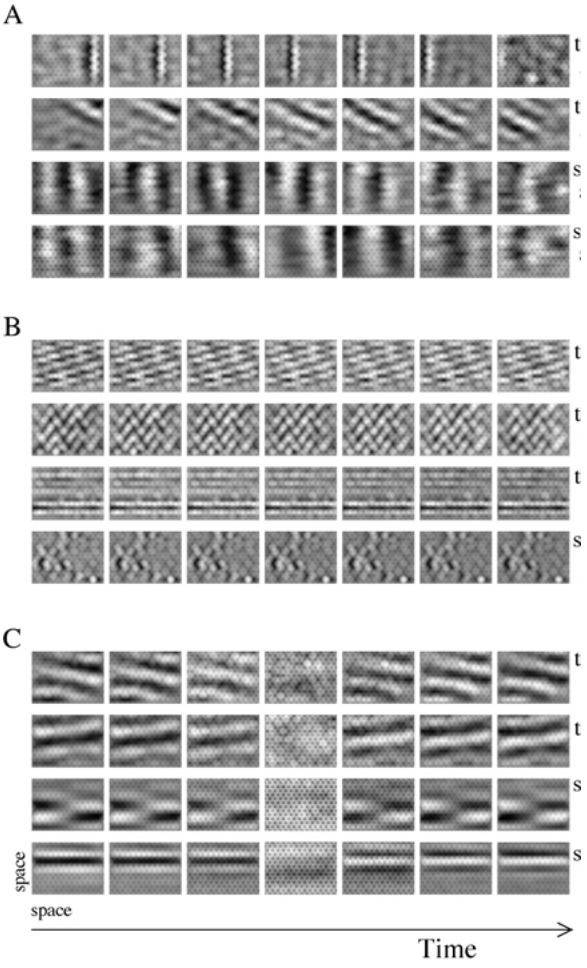

Figure 2. ICFs as a function of convolution time. The ICFs are shown as seven consecutive time frames of 13 × 13 spatial pixels on a hexagonal grid. The grid covers an approximately rectangular area. The ratio of the sides of the rectangle is $\sqrt{3}/2$. Identical results were found for hexagonal areas. Gray value corresponds to zero ICF component, negative values are darker, whereas positive values are lighter. Frames of one line represent one ICF. Spatial properties are shown within each frame, and frames are ordered from left to right according to their temporal indices. A filter image sequence is equal to the optimal input series belonging to the spatiotemporal filter: this image stream can best stimulate the filter. Input dimension is 1183 (7·13·13), PCA compressed dimension is 169 for all frames. Signs t and s denote the database: t: moving gaze (translation), s: constant gaze on image stream. **A:** Four typical space-time non-separable ICFs. Convolution parameter: $\lambda = 0$ (i.e., no convolution). **B:** Four typical filters for convolution parameter around $\lambda = 0.97$. Some of the ICFs represent higher-order structures, show a clear orientation, and have little if any temporal characteristics. The spatial frequency of these ICFs is about twice as large as those of **A**. **C:** Sign-switching ICFs with separable spatiotemporal properties. Convolution parameter: $\lambda \geq 0.9$. The spatial frequency of these ICFs are approximately equal to those of the ICFs of **A**.

There are letters (s and t) on the right-hand side of the individual ICFs denoting whether the ICF was derived from the stream (s) or from translated sampling on the natural scene (t). Four representative filters are shown in Fig. 2A. Each filter can be interpreted as an edge, bar, or wave moving with a fixed velocity perpendicularly to their main axis of orientation. These filters have nonseparable spatiotemporal properties similar to spatiotemporal RFs of cortical simple cells (DeAngelis et al., 1993). The moving structures are visible but are less sharp for the ICFs developed on image stream (moving car) data. As far as the sampling method is considered, solid linear dependence between the sampling distance and the ICF velocity was found for the translating gaze case (not shown on the figures).

Changing the value of the convolution parameter λ but keeping the PCA compressed dimension fixed, we found that for $\lambda \geq 0.6$ the velocity of most of the ICFs becomes approximately zero and the filters become approximately steady (Fig. 2B). These filters have little if any temporal property, have a characteristic spatial frequency (about two times higher than that of the moving filters). Orientation tuning is clearly present in some of these filters. Considering their spatial frequency, these filters cover a larger area than their characteristic period. In turn, these filters are not local edge filters. According to the nomenclature of RFs, these filters can be called complex filters (Sillito, 1979; Henry et al., 1983; Hammond, 1991; Mignard and Malpeli, 1991; Zigmund et al., 1999). Complex filters belonging to uniform direction sampling (translating gaze case) are organized more uniformly than those belonging to the image stream data.

For λ values larger than 0.9, a new type of filter emerged. These filters are sign-switching spatiotemporal filters (Fig. 2C): The filters are nonmoving but are time dependent. The optimal input to the filter is a standing local grating that changes sign. These filters are space-time separable filters. The spatial frequency of these filters is about the same as the spatial frequency of the moving filters. Spatiotemporal RFs, similar to these filters, have been reported in the V1 (DeAngelis et al., 1993).

Olshausen (1996) indicated that both ICA (Bell and Sejnowski, 1995) and sparse coding (Olshausen and Field, 1996) solve essentially the same problem. Hyvärinen et al. (1999) and Hyvärinen (1999a) prove this in broader context and call the joint algorithm sparse code shrinkage. Our PCA/ICA studies can be related to the formulation provided by Olshausen and

Field (1996) by considering in the case of sparse coding a small number of neuronal activities represent a larger number of sensory activities. In turn, *effective compression* occurs when sparse representation is forced (Olshausen and Field, 1996). Assume that ICA/TICA is performed in separated domains of cortical regions, such as in the columns. When the number of LGN inputs to a column of V1 is larger than the number of cortical cells within the column, compression of information takes place in the column. It is then important to study the effect of compression on spatiotemporal ICF characteristics. The dependence of the spatial frequency on the PCA compression ratio and on the sampling distance (the gaze velocity) is shown in Fig. 3. The influence of the sampling distance d and PCA dimension was studied for the moving-gaze experiment at $\lambda = 0$ value. The spatial frequency of the ICFs is a monotone function of both the compressing PCA dimension and the sampling distance. The only exception is the neighborhood of the origin, the region of zero sampling distance, and zero compression. This finding can be visualized as follows. There is a degeneracy in the case of zero gaze velocity; frames of different temporal indices become identical. The result is an effective decrease of the spatiotemporal volume that ICFs may cover. The smaller spatiotemporal region available (one temporal slice instead of seven) constrains the ICFs. In turn, the spatial frequency of the filters becomes high. If the degeneracy is removed, the spatiotemporal volume increases, and the spatial frequency becomes less constrained. The frequency of the filters versus the sampling distance has a minimum because the sampling distance provides a lower bound for the fineness of the structures that can be resolved. The depth of the valley in Fig. 3 is a function of the compression dimension. As expected, the stronger the compression, the more constrained the filters become and, in turn, the less the effect of the sudden increase of the spatiotemporal volume is. For sampling distance greater than 1 (gaze velocity larger than 1 pixel/frame), the ICF spatial frequency depends weakly on the sampling distance.

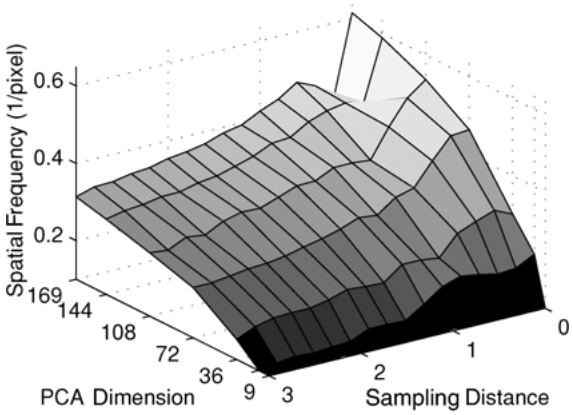

Figure 3. Influence of PCA compression and sampling distance on ICFs. The figure shows the spatial frequency as a function of the sampling distance and the PCA compressed dimension for the moving-gaze experiment in the case of zero temporal convolution. The spatial frequency of each of the emerging ICF is always well characterized, and ICFs have a well defined symmetry axis. The spatial frequency of an ICF was computed by projecting the ICF perpendicular to its symmetry axis, performing Fourier transformation on this projection and estimating the maximal amplitude in the Fourier domain. The average spatial frequency of the emerged set of ICFs is shown. The spatial frequency is a monotone increasing function of the PCA dimension in most regions. However, approaching the zero sampling distance (i.e., zero gaze velocity), nonmonotone behavior can be observed. ICFs at zero gaze velocity are small and exhibit high spatial frequency. For sampling distance greater than 1 (gaze velocity larger than 1 pixel per frame), the ICF spatial frequency depends weakly on the sampling distance.

The relative contributions of the three different filters as a function of the convolution parameter λ are shown in Fig. 4 for the natural scene case. For small λ values ($0 \leq \lambda \leq 0.4$) and for our PCA compression ratio 1183/169, the temporal convolution has negligible influence on the ICFs. These ICFs are similar to those

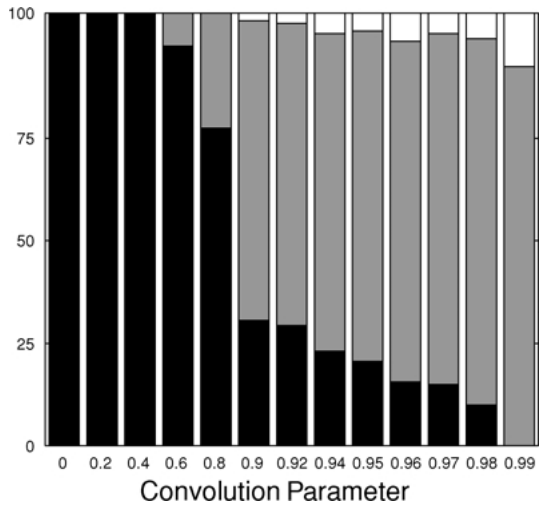

Figure 4. The effect of convolution parameter on filter distribution. The 100% stacked bar shows the ratio of the three filter types as a function of the convolution parameter. The PCA compression ratio is 1183/169. $0 \leq \lambda \leq 0.4$: temporal convolution has negligible influence on the ICFs. $\lambda \geq 0.6$: ICFs with negligible temporal properties and nonlocal characteristics appear. $\lambda > 0.9$: sign-changing ICFs appear. $\lambda \geq 0.99$: nonseparable spatiotemporal filters disappear.

reported by Hateren and Ruderman (1998). If λ becomes greater, then ICFs with negligible temporal properties and nonlocal characteristics appear. $\lambda \simeq 0.9$ results in sign-changing ICFs. Raising the convolution parameter increases the ratio of sign-switching ICFs. For $\lambda \simeq 0.99$, nonseparable spatiotemporal filters disappear. The greatest ratio of separable spatiotemporal filters is about 12% for natural scene and for the type of temporal convolution applied.

4. Discussion

We have extended the works of Olshausen and Field (1996) and Hateren and Ruderman (1998). The extension is motivated by the nature of inputs converging to V1 cells from LGN efferents. There are at least four types of inputs that converge onto principal cells of the V1. The four types of inputs correspond to nonlagged ON and OFF inputs and lagged ON and OFF inputs. The response function of the spatiotemporal receptive field of LGN cells is long lasting (Cai et al., 1997). Dong and Atick (1995) showed that the power spectrum of the response of LGN cells is optimal for natural scenes. That is, LGN cells seem to filter temporal information in an optimal fashion for natural scenes. In our studies one example concerned a natural scene, whereas the other example dealt with highways (i.e., artificial scenes). The two cases have different optimal power spectra, different optimal response functions and, in turn, different optimal temporal smoothing. (For the inverse problem, i.e. for the derivation of the response function from the power spectrum under minimal conditions, see Wimbauer et al., 1997.) In our studies the exponential temporal kernel was chosen for the following reasons: this choice makes the least extension to the work of Hateren and Ruderman (1998), where an infinitesimally sharp exponential kernel was used; the most important effect of temporal smoothing is the mixing of different time indices in a finite temporal window; ICA is invariant for changing signs of the sources, and, in turn, the exponential envelope function is an approximation to the optimal temporal kernel. This approximation is good at local extremes (minima and maxima) of the response function and is poor around null-crossings of the response function. The second reason means that temporal mixing reorders and redirects the most important components to be selected by PCA. In turn, mixing of time indices changes the subspace that will undergo minimization of mutual information (i.e., ICA). We could reproduce all three basic types of receptive fields for both databases cases, in spite of the fact that the type of inputs (natural scene and highway image stream) have different statistical properties (van Hateren and van der Schaaf, 1998). Quantitative comparisons need further work using optimal temporal kernels. It is an intriguing question, whether the response of LGN cells changes for asymmetric inputs as it should be (Gordon et al., 1979; Gordon and Presson, 1982) if information transfer is adaptive at the level of the LGN. This question arises because the statistical properties of visual information filtered by striped cylinders (Gordon et al., 1979) does not fully account for the orientation deprivation found experimentally (Gordon and Presson, 1982).

The emerging ICFs are in good agreement with the properties of the cells' RFs found in the V1. Properties of these ICFs depend strongly on the duration of temporal convolution and on the compressed dimension. The order of appearance of filters as a function of temporal convolution is as follows:

- For small convolution parameter the emerging ICFs exhibit moving Gabor patch-like structure (Fig. 2a). Gabor patches consist of a moving sinusoidal grating windowed by a steady Gaussian envelope. These ICFs are local, i.e. the periodic structure of the ICFs is about one wavelength long. Furthermore they can not be described as the product of temporal and spatial functions: They are space-time nonseparable ICFs alike to those reported by Hateren and Ruderman (1998).
- By increasing the convolution parameter nonmoving complex filters appear (Fig. 2b). These filters are nonlocal—that is, the width of the domain covered by the periodic structure is much larger than the wavelength of the structure. There is a large variety of these filters and the variety depends strongly on the data set.
- Further increase of the convolution parameter gives rise to the appearance of sign-switching filters with separable spatiotemporal properties (Fig. 2c). We were unable to produce sign-switching space-time separable filters without applying temporal convolution in 169 (out of 1183) PCA dimensions.

Therefore, it seems that temporal convolution may be essential to understand and describe these RFs. The increase of the convolution parameter diminishes the ratio of filters with moving grating property. The ratio among the three main filter types of the V1 show strong

dependencies on compression and temporal convolution parameters (Fig. 4) another issue that could be investigated experimentally.

The falsifying question whether information maximization principles can produce complex cells and spatiotemporal receptive fields with both separable and nonseparable spatial and temporal dependencies can be given a positive answer. TICA can provide such filters if temporal convolution originated by properties of LGN cells is taken into account. However, we see no direct explanation why these filters are necessary and how those serve information processing. According to our results on the gradual emergence of these filters, the existence of these filters could originate from the abundance of cells available in V1 *and* the underlying mechanism, which optimizes information transfer. It is also clear from our studies that the appearance of complex cells may produce hyperacuity (Westheimer, 1981; Parker and Hawken, 1987).

Acknowledgments

Helpful discussions with Gábor Szirtes are gratefully acknowledged. This work was supported by Honda Future Technology Research, Germany, and by the Hungarian NSF Grant T32487. Traffic movies were kindly provided by Honda Future Technology Research, Germany, with permission from Werner von Seelen, Ruhr-Universität Bochum, Institut für Theoretische Biologie.

References

Attneave F (1954) Some informational aspects of visual perception. Psychol. Rev. 61:183–193.

Barlow H (1972) Single units and sensation: A neuron doctrine for perceptual psychology? Perception 1:295–311.

Bell A, Sejnowski T (1995) An information-maximization approach to blind separation and blind deconvolution. Neural Comput. 7:1129–1159.

Bell A, Sejnowski T (1997) The "independent components" of natural scenes are edge filters. Vision Res. 37:3327–3338.

Buchsbaum G, Gottschalk A (1983) Trichromacy, opponent colours coding and optimum colour information transmission in the retina. Proc. R. Soc. Lond. B 220:89–113.

Cai D, DeAngelis G, Freeman R (1997) Spatiotemporal receptive field organization in the lateral geniculate nucleus of cats and kittens. J. Neurophysiol. 78:1045–1061.

Calvin W (1999) The MIT Encyclopedia of the Cognitive Sciences. MIT Press, Cambridge, MA. pp. 148–150.

Cover T, Thomas J (1991) Elements of Information Theory. Wiley, New York.

DeAngelis G, Ohzawa I, Freeman R (1993) Spatiotemporal organization of simple-cell receptive fields in the cat's striate cortex. J. Neurophysiol. 69:1091–1117.

DeAngelis G, Ohzawa I, Freeman R (1999) Functional microorganization of primary visual cortex: Receptive-field analysis of nearby neurons. J. Neuroscience 19:1091–1117.

Dong D, Atick J (1995) Temporal decorrelation: A theory of lagged and nonlagged responses in the lateral geniculate nucleus. Network 6:159–178.

Field D (1987) Relations between the statistics of natural images and the response properties of cortical cells. J. Optical Soc. America A4:2379–2394.

Gordon B, Presson J (1982) Orientation deprivation in cat: What produces the abnormal cells? Exp. Brain. Res. 46(1):144–146.

Gordon B, Presson J, Packwood J, Scheer R (1979) Alteration of cortical orientation selectivity: Importance of asymmetric input. Science 204:1109–1111.

Graham R, Knuth D, Patashnik O (1989) Concrete Mathematics: A Foundation for Computer Science. Addison-Wesley, Reading, MA.

Hammond P (1991) On the response of simple and complex cells to random dot patterns: A reply to Skotton, Grosof and de Valois. Vision Res. 31:47–50.

Hateren J, Ruderman D (1998) Independent component analysis of natural image sequences yields spatio-temporal filters similar to simple cells in primary visual cortex. Proc. R. Soc. Lond. B 265:2315–2320.

Haykin S (1994) Neural Networks: A Comprehensive Foundation. Macmillan, New York. pp. 363–370.

Henry G, Mustari M, Bullier J (1983) Different geniculate inputs to B and C cells of cat striate cortex. Exp. Brain Res. 52:179–189.

Hotteling H (1933) Analysis of a complex of statistical variables into principal components. J. Educational Psychol. 24:417–441, 498–520.

Hubel D, Wiesel T (1959) Receptive fields of single neurones in the cat's striate cortex. J. Physiol. 148:574–591.

Hyvärinen A (1999a) Sparse code shrinkage: Denoising of nongaussian data by maximum likelihood estimation. Neural Comput. 11:1739–1768.

Hyvärinen A (1999b) Survey on independent component analysis. Neural Computing Surveys 2:94–128.

Hyvärinen A, Hoyer P, Oja E (1999) Sparse code shrinkage: Denoising by nonlinear maximum likelihood estimation. In: Advances in Neural Information Processing Systems 11 (NIPS*98). MIT Press, Cambridge, MA. pp. 1739–1768.

Hyvärinen A, Oja E (1997) A fast fixed-point algorithm for independent component analysis. Neural Comput. 9:1483–1492.

Lisman J (1999) Relating hippocampal circuitry to function: Recall of memory sequences by reciprocal dentate-CA3 interactions. Neuron 22:233–242.

Lisman J, Idiart M (1995) A mechanism for storing 7 ± 2 short-term memories in oscillatory subcycles. Science 267:1512–1514.

Lőrincz A, Szatmáry B, Kabán A (2000) Independent component analysis of temporally convolved natural image sequences yields spatio-temporal filters similar to cells in primary visual cortex. In: J Bower, ed. Trends in Research: Computational Neuroscience, 2000. Plenum Press, New York.

Mignard M, Malpeli J (1991) Paths of information flow through visual cortex. Science 251:1249–1251.

Olshausen B (1996) Learning linear, sparse, factorial codes. Technical Report AI Memo 1580, CBCL 138, Artificial Intelligence Lab, MIT, Cambridge, MA.

Olshausen B, Field D (1996) Emergence of simple-cell receptive field properties by learning a sparse code for natural images. Nature 381:607–609.

Olshausen B, Field D (1997) Sparse coding with an overcomplete basis set: A strategy employed by V1? Vision Res. 37:3311–3325.

Parker A, Hawken M (1987) Hyperacuity and the visual cortex. Nature 326:105–106.

Pearson K (1901) On lines and planes of closest fit to systems of points in space. Philosophical Magazine 2:559–572.

Saul A, Humphrey A (1990) Spatial and temporal response properties of lagged and nonlagged cells in cat lateral geniculate nucleus. J. Neurophysiol. 64:206–224.

Sillito A (1979) Inhibitory mechanisms influencing complex cell orientation selectivity and their modification at high resting discharge levels. J. Physiol. (Lond.) 289:33–53.

Tailor D, Finkel L, Buchsbaum G (2000) Color opponent receptive fields derived from independent component analysis of natural images. Vision Res. 40:2671–2676.

van Hateren J, van der Schaaf A (1998) Independent component filters of natural images compared with simple cells in primary visual cortex. Proc. R. Soc. Lond. B 265:1–8.

Westheimer G (1981) Visual hyperacuity. Prog. Sensory Physiol. 1:1–37.

Wimbauer S, Wenish O, Miller K, van Hemmen J (1997) Development of spatiotemporal receptive fields of simple cells: I. Model formulation. Biological Cybernetics 77:456–461.

Zigmund M, Bloom F, Landis S, Roberts J, Squire L (1999) Fundamentals of Neuroscinece. San Diego, Academic Press.